Available online at www.sciencedirect.com

ScienceDirect

Nuclear Physics A 973 (2018) 79–88

NUCLEAR PHYSICS A

www.elsevier.com/locate/nuclphysa

Measurement of cross-sections for the ^{93}Nb(p,n)^{93m}Mo and ^{93}Nb(p,pn)^{92m}Nb reactions up to ∼ 20 MeV energy

B. Lawriniang [a], R. Ghosh [a], S. Badwar [a], V. Vansola [b], Y. Santhi Sheela [c], S.V. Suryanarayana [d], H. Naik [e,*], Y.P. Naik [f], B. Jyrwa [a]

[a] *Physics Department, North Eastern Hill University, Meghalaya 793022, India*
[b] *Department of Physics, Faculty of Science, M. S. University of Baroda, Vadodara 390020, India*
[c] *Department of Statistics, Manipal University, Manipal, 576104, India*
[d] *Nuclear Physics Division, Bhabha Atomic Research Center, Trombay, Mumbai 400085, India*
[e] *Radiochemistry Division, Bhabha Atomic Research Center, Trombay, Mumbai 400085, India*
[f] *Product Development Division, Bhabha Atomic Research Centre, Trombay, Mumbai 400085, India*

Received 4 June 2017; received in revised form 23 January 2018; accepted 23 February 2018
Available online 27 February 2018

Abstract

Excitation functions of the ^{93}Nb(p,n)^{93m}Mo and ^{93}Nb(p,pn)^{92m}Nb reactions were measured from threshold energies to ∼ 20 MeV by employing stacked foil activation technique in combination with the off-line γ-ray spectroscopy at the BARC-TIFR Pelletron facility, Mumbai. For the 20 MeV proton beam, the energy degradation along the stack was calculated using the computer code SRIM 2013. The proton beam intensity was determined via the ^{nat}Cu(p,x)^{62}Zn monitor reaction. The experimental data obtained were compared with the theoretical results from TALYS-1.8 as well as with the literature data available in EXFOR. It was found that for the ^{93}Nb(p,n)^{92m}Mo reaction, the present data are in close agreement with some of the recent literature data and the theoretical values based on TALYS-1.8 but are lower than the other literature data. In the case of ^{93}Nb(p,pn)^{93m}Nb reaction, present data agree very well with the literature data and the theoretical values.

Keywords: ^{93}Nb(p,n)^{92m}Mo and ^{93}Nb(p,pn)^{93m}Nb reactions; Stack foil activation technique; Off-line γ-ray spectrometry; Excitation function; TALYS-1.8

* Corresponding author.
E-mail address: naikhbarc@gmail.com (H. Naik).

https://doi.org/10.1016/j.nuclphysa.2018.02.008
0375-9474/

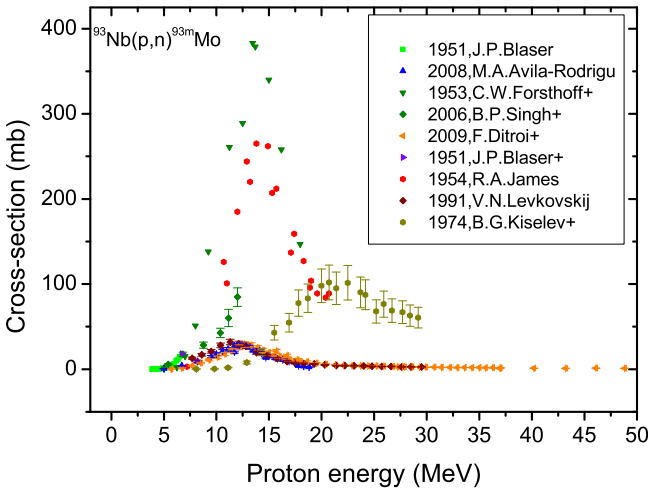

Fig. 1. Excitation function of the ^{93}Nb(p,n)^{93m}Mo reaction from EXFOR database. (For interpretation of the colours in the figure(s), the reader is referred to the web version of this article.)

1. Introduction

The mono-isotopic element niobium is a rare, shiny, malleable, ductile grey white metal with high strength, high melting point (2470°C) and high resistance to corrosion. Niobium is a metal with important technological applications ranging from environmental sciences to nuclear science and accelerator technology [1]. It is use as an alloying element to increase the strength of super alloys since only a small amount of niobium can impart greater strength to other metals, especially those, which are exposed to low temperatures. Due to its superconductive property, niobium is one of the major elements used as superconducting material [2] in different alloys. The alloys of niobium such as NbTi or Nb_3Sn [3] are capable of generating strong magnetic fields and therefore they are used as wires for superconducting magnets and nuclear magnetic resonance instruments in linear accelerator. Thus the charged particle induced reaction cross-sections of niobium are important for accelerator technology. However, the main application of niobium is found in nuclear reactors as structural material due to its exceptionally good physical, chemical properties and low neutron absorption cross-section. Therefore, the neutron induced reaction cross-section data of niobium is important for the design of a nuclear reactor [4]. On the other hand, the knowledge on the excitation function of proton-induced nuclear reactions are of interest for various fields like accelerator technology, for optimising a radioisotope production, for studies of the material behaviours by the charged particle irradiation and also for verification of different models used to explain the reaction mechanism. Since niobium is a mono-isotopic element, its experimental cross-section data can be useful for verification of nuclear reaction theory.

The literature survey based on EXFOR compilation [5] shows that for proton induced reaction on niobium [6–15], a lot of work has been done on the measurements of ^{93}Nb(p,n)^{93m}Mo and ^{93}Nb(p,pn)^{92m}Nb reaction cross-sections. However, the literature data show many discrepancies and poor agreement between them particularly for the ^{93}Nb(p,n)^{93m}Mo reaction, which have a wide variation from one another. These discrepancies in the magnitude of cross-section values from literature data are evident in Fig. 1 where at the same proton energy, the data reported by dif-

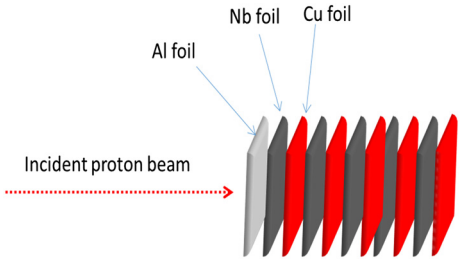

Fig. 2. Schematic arrangement of the metal foils in stacked foil activation technique.

ferent group of experimentalists do not agree. Fig. 1 revealed that the ^{93}Nb(p,n)^{93m}Mo reaction cross-section data by Blaser et al. [6], Forsthoff et al. [7], James [8] and Kiselev et al. [9] show higher cross-section values than other experimental data. This may be due to the older measurements when the HPGe detector was not available. Thus in the present work, a study of activation cross-sections of proton induced reactions on niobium was done with the aim of applications in accelerator, reactor technology and for obtaining a more reliable cross-section data. We have measured the ^{93}Nb(p,n)^{93m}Mo and ^{93}Nb(p,pn)^{92m}Nb reaction cross-sections (σ_R) at the proton energies from threshold energy up to 18.63 MeV using stacked foil activation technique in combination with the off-line γ-ray spectroscopy [16]. The ^{93}Nb(p,pn)^{92m}Nb and ^{93}Nb(p,n)^{93m}Mo reaction cross-sections from the present work were compared with literature data [6–15] to look for the discrepancies.

2. Experimental details

The experiment was performed by using the 14 UD BARC-TIFR (Bhabha Atomic Research Centre and Tata Institute of Fundamental Research) Pelletron facility at Mumbai, India. The proton beam main line at 6 m above the analysing magnet of the Pelletron facility was used to utilise the maximum proton current from the accelerator. At this port, the terminal voltage is regulated by generating voltage mode (GVM) using a terminal potential stabiliser. Further, we use a collimator of 6 mm diameter before the target.

A conventional stack-foil activation technique was used in the experiment as done by most of the authors [10–13]. For this purpose, high purity (> 99.99%) niobium metal foils of 91 µm thickness were used as the target for irradiation. Similarly, high purity (> 99.99%) copper foils of 103 µm thickness were also included in the stacks so as to monitor the proton beam energy as well as to serve as the energy degrader along the stack. The thickness of each foil was determined from the standard relation of mass, area, density and thickness after the precise measurements of their dimensions and mass of the samples. The maximum uncertainty in the thickness was less than 0.5%. The sizes of the niobium foils were 0.7×0.7 cm^2, whereas those of copper foils were 0.8×0.8 cm^2. A stack consisting of five niobium foils each separated by copper foils were arranged in the order Al-Nb-Cu-Nb-Cu-Nb-Cu-Nb-Cu-Nb-Cu. The thickness of aluminium foil was $\sim$ 108 µm. A schematic arrangement of the stack is shown in Fig. 2. The copper monitor foils were irradiated simultaneously with the niobium foils and the ^{nat}Cu(p,x)^{62}Zn reaction was used as a proton flux monitor.

The stack of foils was irradiated with a proton beam of 20 MeV from the Pellatron facility for 30 minutes at a beam current of 50 nA. During the irradiation, the beam intensity was kept constant and it was checked that equal areas of monitor and target foils intercepted the beam.

The energy of the incident proton beam decreases, as it passes through the stack and so the successive foils of the stack were irradiated with incident particles of different energies. The γ-ray activity measurements of the irradiated samples were started after a sufficient cooling time from the end of irradiation to avoid the disturbance of the overlapping γ-lines emitted by the short-lived radionuclides. After a considerable cooling time (7.88 hours to 14 days for niobium and 8.35 hours for copper foils), the irradiated samples were mounted on different Perspex plates of particular size, which fits on the shelf of the sample stand.

The γ-ray activities of the irradiated Nb and Cu foils were measured by off-line γ-ray spectrometric technique, using a 20% HPGe detector connected to a PC based 4K channel analyser. The energy and efficiency calibration of the HPGe detector was done using a standard ^{152}Eu source [17,18] of known strength. The detection efficiencies as a function of γ-ray energy for the detector were obtained at various source to detector distances. The resolution of the detector had a FWHM of 1.8 keV at 1332.5 keV γ-ray peak of ^{60}Co. The γ-ray counting of the irradiated samples were done in pulse height analysis (PHA) mode in the order of last foil to the first foil based on the proton energy faced by those metal foils. The coincidence summing error was avoided by placing those irradiated samples at a suitable distance of 10–20 cm from the end-cap of the detector. The dead time of the detector system was always kept below 5% to avoid pile up effect. This was observed based on the difference of real time and live time as well as based on the γ-ray counting software. Three set of γ-ray counting were done for each niobium samples. The monitor foils were measured twice in order to find out any mistake in data analysis for more accurate evaluation of cross-section. The residual nuclei of interest such as ^{92m}Nb, ^{93m}Mo from the ^{93}Nb(p,x) reactions and the ^{62}Zn from the ^{nat}Cu(p,x) monitor reaction were identified by their characteristic γ-lines as well as by their measured half-lives. The decay and spectrometric characteristics of the investigated isotopes were taken from NuDat database [19] and are summarised in Table 1.

3. Data analysis

The threshold energies of the ^{93}Nb(p,pn)^{92m}Nb and ^{93}Nb(p,n)^{93m}Mo reactions as well as of the ^{nat}Cu(p,x)^{62}Zn monitor reaction were calculated using the Qtool [20] taking into account the excitation energy of the metastable states and are shown in Table 1. The proton beam energy degradation along the stack was calculated using the computer code SRIM 2013 of Ziegler [22] or a new method developed by Fisichella et al. [23]. However, we have followed the same procedure [22] for the calculation of proton energy degradation as done by others [9–15] to compare the present data with their data. Thus the proton beam energy degradation along the stack was calculated by SRIM 2013 code [22] with initial incident energy of 20 MeV on the aluminium foil. After the energy loss in the aluminium foil, the proton energy for the first niobium and first copper foils are 18.63 and 17.34 MeV, respectively. The calculated proton energies along with their uncertainties for each Nb target foils are given in Table 2. It can be seen from Table 2 that the uncertainties of proton energies are and 0.53 and 1.07 MeV for the first and fourth Nb target foils, respectively. However, the uncertainties of proton energies in the Cu foils are not given in Table 2. The proton beam intensity i.e. the proton flux was determined from the first copper foil of the stack using the ^{nat}Cu(p,x)^{62}Zn monitor reaction with known cross-section taken from IAEA database [24]. The loss of proton flux along the stack was negligible. The proton flux was considered constant in the calculation of ^{93}Nb(p,pn)^{92m}Nb and ^{93}Nb(p,n)^{93m}Mo reaction cross-sections as a function of proton energy for each foil of the stack.

Table 1
Nuclear spectroscopic data for the radionuclides from the $^{nat}Cu(p,x)^{62}Zn$, $^{93}Nb(p,n)^{93m}Mo$ and $^{93}Nb(p,pn)^{92m}Nb$ reactions.

Nuclide	Half-life	Decay mode	γ-Ray energy E_γ (keV)	γ-Ray intensity I_γ (%)	Production route	Threshold energy (MeV)	Spin and parity
^{62}Zn	9.186 h	ε (100%)	548.35	15.3	$^{63}Cu(p,2n)$	13.47	0^+
			596.56	26.0			
^{92m}Nb	10.15 d	ε (100%)	934.44	99.15	$^{93}Nb(p,pn)$	9.06	2^+
^{92g}Nb	3.47×10^7 y	ε (100%)	934.5	74.0	$^{93}Nb(p,pn)$	8.93	7^+
		β^+ (< 0.05%)					
^{93m}Mo	6.85 h	IT (99.88%)	263.05	57.4	$^{93}Nb(p,n)$	3.65	$(21/2)^+$
		ε (0.12%)	684.69	99.9			
			1477.14	99.1			
^{93g}Mo	4.0×10^3 y	ε (100%)	–	–	$^{93}Nb(p,n)$	1.20	$(5/2)^+$

Table 2
Experimental cross-sections for the ^{93}Nb(p,n)^{93m}Mo and ^{93}Nb(p, pn)^{92m}Nb reactions.

Proton energy (MeV)	^{nat}Cu(p,x)^{62}Zn reaction cross-section σ (mb) [24]	Proton flux (p/cm^2)	^{93}Nb(p,n)^{93m}Mo reaction cross-section σ_R (mb)	^{93}Nb(p,pn)^{92m}Nb reaction cross-section σ_R (mb)
8.60 ± 1.07	37.25	4.399×10^{11}	6.50 ± 0.46	–
12.54 ± 0.70			24.07 ± 0.49	2.00 ± 0.63
15.79 ± 0.61			12.73 ± 0.95	30.32 ± 1.44
18.63 ± 0.53			5.43 ± 0.42	64.74 ± 1.98

It can be seen from Table 1 that the radionuclide ^{92}Mo has ground and metastable states. The ground state radionuclide (^{93g}Mo) has a long half-life of 4.0×10^3 years whereas the metastable state radionuclide (^{93m}Mo) has a half-life of 6.85 hours. The metastable state was identified by the γ-lines of 263.05 keV (57.4%), 684.69 keV (99.8%) and 1477.14 keV (99.1%), which were used for the determination of reaction cross-section (σ_R). Since the radionuclide ^{93m}Mo decays by both IT (99.88%) and electron capture (0.12%), the γ-lines are only from the internal energy transition. For the radionuclide ^{92}Nb, both the ground and the metastable states have the same γ-ray energy but the half-life of the ground state is extremely long ($T_{1/2} = 3.47 \times 10^7$ y). In our experiment, the measured photo-peak area of ^{92}Nb is from short counting time, therefore the measured cross-section is only of the metastable state (^{92m}Nb). The radionuclide ^{92m}Nb has a half-life of 10.15 days and identified by the strong γ-line of 934.44 keV, which was used to determine the reaction cross-section (σ_R).

The observed photo-peak area (A) of the induced activity for the nuclide of interest was obtained from the gross photo-peak area after subtracting the Compton background. From the net photo-peak areas of the identified γ-rays of the residual nuclei of interest, their decay rates and the measured beam intensity, the cross-section (σ_R) of the investigated nuclear reactions were determined using the following activation formula [25]:

$$\sigma_R = \frac{A\lambda\left(\frac{CL}{LT}\right)}{N\phi I_\gamma \varepsilon \left(1 - e^{-\lambda T_i}\right) e^{-\lambda T_c}(1 - e^{\lambda CL})} \tag{1}$$

where λ is the decay constant ($\lambda = \ln 2 / T_{1/2}$) of the reaction product of interest with a half-life $T_{1/2}$ N is the number of target atoms Φ is the proton flux from the monitor reaction I_γ is the branching intensity of the γ-ray energy ε is its detection efficiency of the γ-ray energy T_i, T_c, CL and LT are the irradiation, cooling, clock and live times respectively.

The detection efficiency (ε) of the detector, the γ-ray intensity and the half-lives of the radioisotopes were taken into account for the calculation of reaction cross-section.

4. Results and discussion

The cross-sections (σ_R) for the ^{93}Nb(p,n)^{93m}Mo and ^{93}Nb(p,pn)^{92m}Nb reactions at different proton energies determined from the present work are given in Table 2. The uncertainties associated to the measured cross-sections are based on the repeated measurements. The overall uncertainty is the quadratic sum of both statistical and systematic uncertainties. The random uncertainty in the observed activity is primarily due to counting statistics, which is estimated to be 2.1–3.7%. This can be determined by accumulating the data for an optimum time period that depends on the half-life of the nuclide of interest. The systematic uncertainties are due to uncertainty in the proton flux estimation ($\sim$ 4.4–19.6%), the irradiation time ($\sim$ 0.5%), the

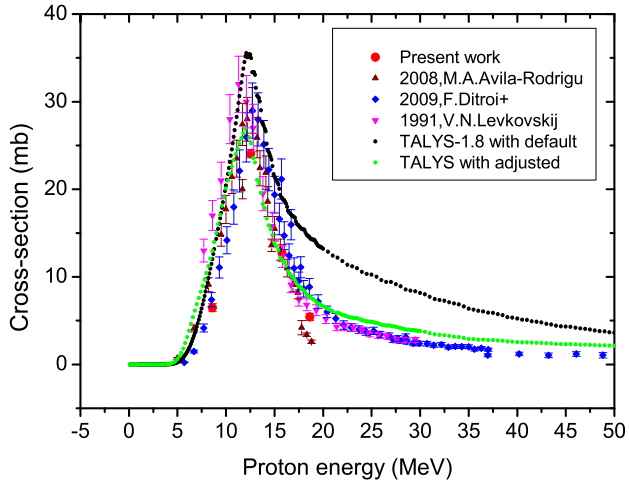

Fig. 3. Excitation function of the ^{93}Nb(p,n)^{93m}Mo reaction excluding some of the literature data.

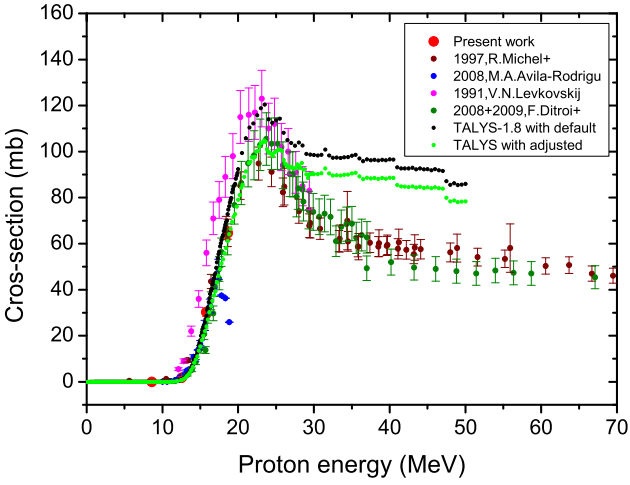

Fig. 4. Excitation function of the ^{93}Nb(p,pn)^{92m}Nb reaction.

detection efficiency calibration ($\sim$ 3.7%), the half-life of the reaction products and the γ-ray abundances ($\sim$ 2%) as reported in the literature [19]. Thus, the total systematic uncertainty is about $\sim$ 6.1–20.1%. The overall uncertainty in the cross-sections was found to be in the range of 6.5–20.4%, coming from the combination of a statistical uncertainty of 2.1–3.7% and a systematic uncertainty of 6.1–20.1%.

It can be seen from Table 2 that within the proton energy of 18.63 MeV, the ^{93}Nb(p,n)^{93m}Mo reaction cross-section increases from the threshold energy to a particular value and then decreases, whereas that of ^{93}Nb(p,pn)^{92m}Nb reaction shows only increasing trend. In order to examine this, the cross-sections for the ^{93}Nb(p,n)^{93m}Mo and ^{93}Nb(p,pn)^{92m}Nb reactions from the present work and literature data available in EXFOR [5] at different proton energies were shown in Figs. 3 and 4. For comparison, the cross-sections for the ^{93}Nb(p,n)^{93m}Mo and

^{93}Nb(p,pn)^{92m}Nb reactions were also calculated theoretically using the computer code TALYS-1.8 [21] with default and adjusted parameters.

4.1. ^{93}Nb(p,n)^{93m}Mo reaction cross-section

As mentioned earlier and shown in Fig. 1, there are discrepancies in the magnitude of ^{93}Nb(p,n)^{93m}Mo reaction cross-section data in literature [6–14]. At the same proton energy, the data from the different group of experimentalists has a great variation. In particular, the ^{93}Nb(p,n)^{93m}Mo reaction cross-section reported by Blaser et al. [6], Forsthoff et al. [7], James [8], Kisilev et al. [9] and Singh et al. [10] are significantly higher than the other literature data [10–14]. This is most probably because the data reported by Blaser et al. [6], Forsthoff et al. [7] and James [8] are measurements from a time when the HPGe detector was not available. James [8] has determined the ^{93}Nb(p,n)^{93m}Mo reaction cross-section within the proton energy of 8.1–29.2 MeV by using the Geiger Muller tube and Scintillation detector. Similarly, Forsthoff et al. [7] have determined the ^{93}Nb(p,n)^{93m}Mo reaction cross-section within the proton energy of 5.02–17.95 MeV using a β-detector. On the other hand, Kisilev et al. [9] and Singh et al. [10] have measured the ^{93}Nb(p,n)^{93m}Mo reaction cross-section within the proton energy of 8.1–29.1 MeV and 5.4–12 MeV using the activation and γ-ray spectrometric technique with Ge(Li) or HPGe detector. The cross-section determined by Kisilev et al. [9] has a peak cross-section shift to higher proton energy. This may be because of the improper proton energy degradation calculation, which must have causes the use of improper ^{nat}Cu(p,x)^{65}Zn monitor reaction cross-section and in turn results in higher and peak cross-section shift to higher proton energy. However, the reason for higher ^{93}Nb(p,n)^{93m}Mo reaction cross-section values obtained by Singh et al. [10] is not clearly known.

In view of all the above facts, the ^{93}Nb(p,n)^{93m}Mo reaction cross-section from the present work were shown in Fig. 3 and compared with the theoretical values from TALYS-1.8 [21] as well as with the similar literature data [12–14], which are consistent to each other. It can be seen from Fig. 3 that the present work agree well with the measured data reported by Avila Rodrigues et al. [12], Ditroi et al. [13] and Levkovski [14]. All these data which are in good agreement with our data, have been measured by using a solid state detector either with a GeLi or HPGe detector. It can also be seen from Fig. 3 that the theoretical values from TALYS-1.8 [21] follow a similar trend but are higher than the experimental data above the proton energy of 15 MeV. This may be because of the use of default parameters in the theoretical calculations using TALYS-1.8 [21]. In this context, we again performed the theoretical calculation of cross-section for the ^{93}Nb(p,n)^{93m}Mo reaction by using TALYS-1.8 with adjusted optical model parameters within the proton energy range from threshold to 50 MeV to obtain a better fit to the literature and present data.

In the present calculation, we have adjusted only one parameter (v_1) of the real volume term of the optical model as given by Konig and Delaroche [26] to obtain the best fit to the data. In TALYS-1.8, the value of v_1 can be adjusted by using the keyword v_1 adjust with which its standard value is multiplied. The default value of v_1 is 1 whereas we have used the adjusted value of 4.5.

The ^{93}Nb(p,n)^{93m}Mo cross-section values obtained from TALYS-1.8 based on adjusted parameters are in a good agreement with the experimental values and literature data over the entire interested energy range. Thus the experimental ^{93}Nb(p,n)^{93m}Mo reaction cross-section gives a good test of the optical model.

4.2. $^{93}Nb(p,pn)^{92m}Nb$ reaction cross-section

Fig. 4 shows the comparison of the ^{93}Nb(p,pn)^{92m}Nb reaction cross-section from the present work with those of earlier measurements from literature and theoretical values from TALYS-1.8 [21] with default and adjusted parameters. It can be seen from Fig. 4 that the present data agree well with the existing literature data of Ditroi et al. [11,13], Avila Rodrigues et al. [12] and Michel et al. [15] but are lower than the data of Levkovski [14]. It can also be seen from Fig. 4 that up to a proton energy of 25 MeV, the measured data from present work and literature [11–13, 15] agree well with the theoretical values from TALYS-1.8 [21] code based on both default and adjusted parameters [26]. However, up to a proton energy of 25 MeV, the data of Levkovski [14] are higher than the theoretical values based on the TALYS-1.8 [21,26]. Above the proton energy of 25 MeV, all the literature data [11–15] are lower than the values from TALYS-1.8 based on both default and adjusted parameters.

The comparison of experimental cross-sections with those of theoretical values for the ^{93}Nb(p,n)^{93m}Mo and ^{93}Nb(p,pn)^{92m}Nb reactions gives a good test of TALYS code and the optical model parameters. The above observation also indicates that when a compound nucleus emits only one neutron then adjusting the value of v_1 is sufficient to reproduce the experimental results, which was observed from the ^{93}Nb(p,n)^{93m}Mo reaction cross-section. On the other hand, when the compound nucleus emits a proton in addition to neutron, then adjusting the value of v_1 is sufficient to reproduce the experimental results only up to a proton energy of 25 MeV, which was observed from the ^{93}Nb(p,pn)^{92m}Nb reaction cross-section. Above the proton energy of 25 MeV, adjustment of other parameters besides v_1 is very much necessary for a reaction where emission of proton in addition to neutron takes place from the compound nucleus.

5. Conclusions

The ^{93}Nb(p,n)^{93m}Mo and ^{93}Nb(p,pn)^{92m}Nb reaction cross-sections at the proton energies of 8.60, 12.54, 15.78 and 18.63 MeV have been experimentally determined and theoretically calculated as a function of proton energy using the computer code TALYS-1.8. The ^{93}Nb(p,n)^{93m}Mo reaction cross-sections from the present work and similar literature data within the proton energy of 50 MeV are in good agreement with the theoretical values of TALYS-1.8 based on adjusted parameter of optical model. On the other hand, the ^{93}Nb(p,pn)^{92m}Nb reaction cross-section from the present work and similar literature data are in good agreement with the theoretical values of TALYS-1.8 within the proton energy of 25 MeV but not at higher proton energy even with the adjusted optical model parameter. Thus the experimental results will be useful to upgrade theoretical codes, for the estimation of the activity for future accelerator development and for isotope production.

Acknowledgements

We would like to express our sincere thanks to the staffs of Tata Institute of Fundamental Research (TIFR), Mumbai for their excellent operation of the accelerator and for providing the proton beam for our experiment. One of the authors (B. Lawriniang) is also thankful to University Grant Commission (UGC) for providing the financial assistance for her PhD work.

References

[1] H. Padamsee, RF Superconductivity for Accelerators, John Wiley & Sons, 1998.

[2] P.N. Lebedev, Sov. Phys. JETP 30 (1970) 1068.
[3] S. Posen, D.L. Hall, Supercond. Sci. Technol. 30 (2017) 1.
[4] A.V. Nikulina, Met. Sci. Heat Treat. 45 (2003) 287.
[5] IAEA-EXFOR Experimental nuclear reaction data base, http://www.nds.iaea.org/exfor.
[6] J.P. Blaser, F. Boehm, P. Marmier, P. Scherrer, Helv. Phys. Acta 24 (1951) 24.
[7] C.W. Forsthoff, R.H. Goeckermann, R.A. Naumann, Phys. Rev. 90 (1953) 1004.
[8] R.A. James, Phys. Rev. 93 (1954) 288.
[9] B.G. Kiselev, N.R. Faizrakhmanova, in: Conf. Nucl. Spectr. Nucl. Struct., Kharkov, 1974, p. 356.
[10] B.P. Singh, Manoj K. Sharma, M.M. Musthafa, H.D. Bhardwaj, R. Prasad, Nucl. Instrum. Methods A 562 (2006) 717.
[11] F. Ditrói, S. Takács, F. Tárkányi, M. Baba, E. Corniani, Y.N. Shubin, Nucl. Instrum. Methods B 266 (2008) 5087.
[12] M.A. Avila-Rodriguez, J.S. Wilson, M.J. Schueller, S.A. McQuarrie, Nucl. Instrum. Methods B 266 (2008) 3353.
[13] F. Ditrói, A. Hermanne, E. Corniani, S. Takács, F. Tárkányi, J. Csikai, Y.N. Shubin, Nucl. Instrum. Methods B 267 (2009) 3364.
[14] V.N. Levkovski, Activation Cross Sections by Protons and Alphas, Inter-Vesi, Moscow, 1991.
[15] R. Michel, R. Bodemann, H. Busemann, R. Daunke, M. Gloris, H.J. Lange, B. Klug, A. Krins, I. Leya, M. Lüpke, S. Neumann, H. Reinhardt, M. Schnatz-Büttgen, U. Herpers, T. Schiekel, F. Sudbrock, B. Holmqvist, H. Condé, P. Malmborg, M. Suter, B. Dittrich-Hannen, P.W. Kubik, H.-A. Synal, D. Filges, Nucl. Instrum. Methods B 129 (1997) 153.
[16] I. Rittersdorf, Gamma Ray Spectroscopy, Nucl. Engineering & Radiological Sciences, 2007.
[17] I.A. Alnour, H. Wagiran, N. Ibrahim, S. Hamzah, W.B. Siong, M.S. Elias, AIP Conf. Proc. 38 (2014) 1584.
[18] A.W. Tyler, Phys. Rev. 56 (1939) 125.
[19] NuDat 2.7β, National Nuclear Data Center, Brookhaven National Laboratory, 2011, http://www.nndc.bnl.gov/.
[20] Qtool: calculation of reaction Q-values and threshold, Los Alamos National Library, http://cdfe.sinp.msu.ru/services/calc_thr/calc_thr.html.
[21] A.J. Koning, S. Hilaire, S. Goriely, TALYS user manual, A nuclear reaction program, NRG-1755 ZG PETTEN, The, Netherlands, 2015.
[22] J.F. Ziegler, Nucl. Instrum. Methods B 219 (2004) 1027, http://www.srim.org/.
[23] M. Fisichella, A.C. Shotter, A. Di Pietro, P. Figuera, M. Lattuada, C. Marchetta, V. Privitera, L. Romano, C. Ruiz, M. Zadro, Phys. Rev. C 92 (2015) 064611.
[24] S.M. Qaim, F. Tárkányi, P. Obložinskỳ, K. Gul, A. Hermanne, M.G. Mustafa, F.M. Nortier, B. Scholten, Yu. Shubin, S. Takács, Y. Zhuang, Charged Particle Cross-Section Database for Medical Radioisotope Production: Diagnostic Radioisotopes and Monitor Reactions, Vienna, IAEA-TECDOC-1211, Data updated in January 2007, available at, http://www-nds.iaea.org/medical/monitor_reactions.html, 2001.
[25] G. Gilmore, J.D. Hemingway, Practical Gamma-Ray Spectrometry, John Wiley and Sons, England, 1995, p. 17.
[26] A.J. Koning, J.P. Delaroche, Local and global optical models from 1 keV to 200 MeV, Nucl. Phys. A 713 (2003) 231.